doi:10.2533/chimia.2022.212 Chimia 76 (2022) 212–222

From Synthesis to Microstructure: Engineering the High-entropy Ceramic Materials of the Future

Amy J. Knorpp*, Jon G. Bell*, S. Huangfu*, and M. Stuer*

Abstract: Sintering and microstructural development in ceramics has long been studied in a two-dimensional grain size-density space, with only texture (*i.e.* deviation of grain orientation from random) used to gain first insights into additional parametric spaces. Following an increased interest for grain boundary engineering and a deeper understanding of dopant effects on sintering and grain boundaries, the theory of complexion transitions for ceramics has been introduced over the last decade, providing a new base for advanced microstructure engineering in ceramics. With emergence of high-entropy ceramics over the last five years, the combination of both yields new grounds for exploration and engineering of functional ceramic materials of the future.

Keywords: High-entropy ceramics · Microstructural engineering · Powder synthesis

Dr. Amy J. Knorpp is a post-doctoral researcher at the High Performance Ceramics Laboratory at Empa. Before acquiring a PhD from ETH Zürich, she studied Civil and Environmental Engineering at Stanford University, USA followed by a few years of industry experience in performance minerals. After completion of her PhD, she joined Empa in 2020 and has been working on powder synthesis, processing and sintering of ceramics. Her current research interests are on shape, phase and crystallinity controlled synthesis of high-entropy ceramics for methanation and microstructural engineering of functional ceramics.

Dr. Jon G. Bell is a scientist within the High Performance Ceramics Laboratory at Empa. After completion of his PhD in Physical Chemistry from Newcastle University, UK, he gained several years of gas separation process experience in the UK industrial sector. Before joining Empa in 2019 with an MSCA Fellowship under H2020, he worked at as a post-doctoral researcher, investigating sorption processes within metal organic frameworks and porous coordination polymers. His current research interests include studying the role of microstructure and defect chemistry on the electrochemical and gas sensing properties of electroceramics.

Dr. Shangxiong Huangfu is a post-doctoral researcher at the High Performance Ceramics Laboratory at Empa. He studied experimental physics and acquired his PhD in physical properties characterization of crystalline materials at the University of Zurich in 2020. Before that, he obtained his master's degree in crystalline material science at the Chinese Academy of Science. His current research interests are on single crystal growth, superconductivity, as well as electronic and magnetic properties of crystalline materials.

Dr. Michael Stuer is Head of the Nanopowders and Ceramics group at the High Performance Ceramics Laboratory at Empa. He studied Material Science and acquired his PhD in Powder Technology and Ceramics at EPFL in Lausanne on a joint project together with Stockholm University. After working as a Research Engineer and later as a Technology and Innovation Manager in different Swiss industrial sectors, he joined Empa in 2019. Since 2020, he is also lecturer at EPFL. Studying powder synthesis, processing and sintering for microstructural engineering to understand structure–property relationships, he works to combine different approaches to bridge the gap between idealized system descriptions and their statistical relevance in real material systems.

1. Introduction

The achievement of transparent ceramics,[1–4] especially transparent alumina where the birefringence calls for texture or fine grain sizes,[5,6] ended a decades long cycle of ceramic powder synthesis, processing and sintering research strongly focused on two microstructural parameters: density and grain size. This important achievement, since then applied to various ceramics and processing routes,[7–14] established an important baseline required to bring attention to the advanced microstructural engineering of ceramics, and more particularly to grain boundary engineering.[15–17] Indeed, with many functional ceramic properties such as the positive temperature coefficient of resistivity being grain boundary dependent,[18] the controlled engineering of the grain boundary character distribution enables new ways to further improve and target material properties for their respective applications, beyond

*Correspondence: Dr. A.J. Knorpp, E-mail: amy.knorpp@empa.ch; Dr. J.G. Bell, E-mail: jon.bell@empa.ch; Dr. S. Hunangfu, E-mail: shangxiong.huangfu@empa.ch; Dr. M. Stuer, E-mail: michael.stuer@empa.ch
High Performance Ceramics Laboratory, Swiss Federal Laboratories for Materials Science and Technology (Empa), CH-8600 Dübendorf, Switzerland
All authors contributed equally to the manuscript

conventional microstructure engineering mostly focused on grain size, texture and/or density.

Prior to grain boundary engineering, flawless powder processing and shaping is a prerequisite, as agglomerates and green body inhomogeneities in general may interfere with the microstructural development during sintering,[19,20] Beside texturing through templated grain growth and aniso-metric or -tropic particle alignment, strongly relying on the powder processing strategy and grain growth,[21–23] the doping strategy and sintering cycle parameters are the most commonly used tools to modify the microstructural development during sintering.[24,25] However, when grain growth is to be strictly minimized, the importance of an additional parameter increases: the initial powder morphology. Indeed, the facets of the particles may form the initial grain boundaries and thus affect the initial grain boundary character distribution.

Experimental observation showed that two-step sintering protocols could successfully be implemented to prevent (abnormal) grain growth.[26–28] Through Cs-corrected high resolution transmission electron microscopy of doped ceramics,[29] as well as atomistic modelling of doped surfaces and grain boundary interfaces,[30–32] the awareness and theoretical description of doping effects on sintering have improved over the last decade. Beside doping effects on diffusion,[33] grain boundary and surface energies[30,31] as well as the relation between grain growth versus densification,[34] dopants may induce complexion transitions at the grain boundaries.[15,35–38] In contrast to phase transitions, complexion transitions also depend on the local atomic structure, namely the mismatch angles between the adjacent grains and their separation plane.[15,38] Since complexion transitions may induce abnormal grain growth, change the mobility and the excess energy of the grain boundaries, they play an essential role in successful grain boundary engineering. Considering the potential need for substantial grain growth, the availability of finer crystalline nanopowders[40,41] will provide the means to achieve both grain boundary and microstructure engineering. As novel ceramic materials emerge, incorporating this knowledge, like grain boundary engineering through doping and complexion transitions, illustrated above with the example of alumina, is important for the discovery and optimization of new materials. Grain boundaries playing a significant role for many properties and applications, engineering thereof has to be considered from the onset to facilitate scientific and technological progress. This is also the case for high-entropy ceramics (HEC), which – due to their recent discovery[42] – remain a novel class of ceramics, largely left to be explored and documented in literature. With how one synthesizes, sinters, and shapes HECs in such early development, a wholistic assessment will be key to rapidly increase our understanding on how to control microstructures for HECs, and explore their effects on the material properties. In this work, we highlight current strategies in making HECs and summarize what is known to date about control of their microstructures with an eye toward future research directions. Finally, by selecting specific applications as case studies, we show the potential and unexplored space of grain boundary engineering for novel HECs.

1.1 *Introduction to High-entropy Materials*

New materials that have multiple degrees of freedom to engineer the structure and its properties have led to important paradigm shifts in material design from the Bronze Age to the modern day. Many historically important discoveries from bronze to stainless steel have been the result of substituting or utilizing different elements into various materials' structure to enhance properties. In 2004, the work of Cantor[43] and Yeh[44] began to explore the extremes of the substitution of elements into alloys which then led to the advent of a new material class called high-entropy alloys (HEAs). The name, HEAs, is derived from the increasing number of elements randomly distributed in a structure and the resulting increased intrinsic disorder or configurational entropy. To define a material as high-entropy, there are two different metrics currently utilized: *i)* a composition of five or more elements that are equiatomic with each other, or *ii)* a calculated configurational entropy of 1.5 R or more where R is the gas constant. Additionally, the incorporation of the different multiple elements must be random and homogenous and result in a single phase. The definitions and concepts developed for high-entropy alloys have served as the basis to discover and identify other classes of high-entropy materials (HEMs). Not only has the field of HEAs grown dramatically in the last two decades, but several new classes of high-entropy materials have been discovered, as shown in Fig. 1.

What has driven this search for high-entropy materials are the unique properties that arise from local compositional disorder but in a long-range ordered structure. In alloys and by extension other high-entropy materials, four core effects of the high-entropy configuration have been identified: i) cocktail effects of multiple elements, ii) sluggish diffusion effects, iii) severe lattice distortions, and finally iv) high-entropy effects that effect solubility limits and stability. Unique and promising properties arise from these core effects that hold promise for a range of applications including catalysis, optical materials, superconductors, energy storage, and coatings.

1.2 *High-entropy Ceramics*

With the discovery of high-entropy oxides,[42] nitrides,[45] borides,[46] carbides,[45] and silicides,[47] the field of high-entropy ceramics (HECs) was founded. High-entropy oxides (HEOs) have drawn particular interest because there is a diverse range of crystal structures that can have a high-entropy configuration. Within HEOs alone, high-entropy forms of rock-salt,[42] fluorite,[48] spinel,[49] perovskite,[50,51] magnetoplumbite,[52] pyro-chlore,[53] garnet[54] and sesquioxide[48,55] can exist as shown in Fig. 2.

In an HEO system that contains multiple cations, an entropically stabilized multi-phase to single-phase transition will oc-

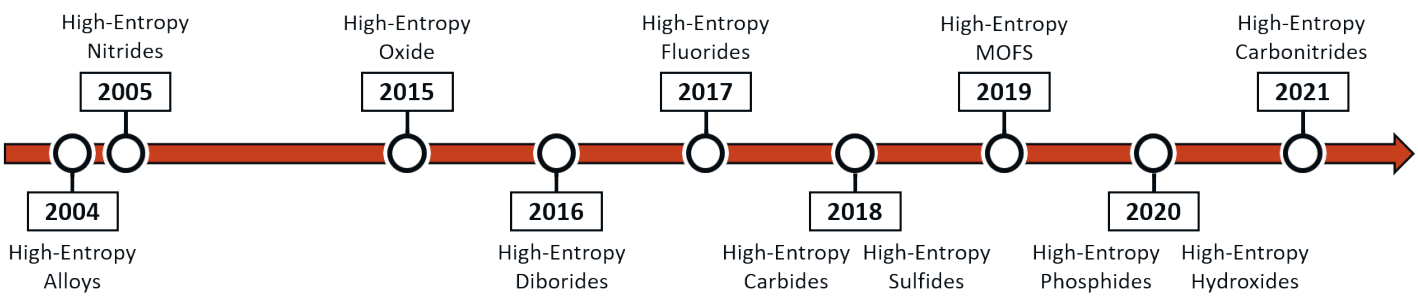

Fig. 1. Timeline of high-entropy materials.

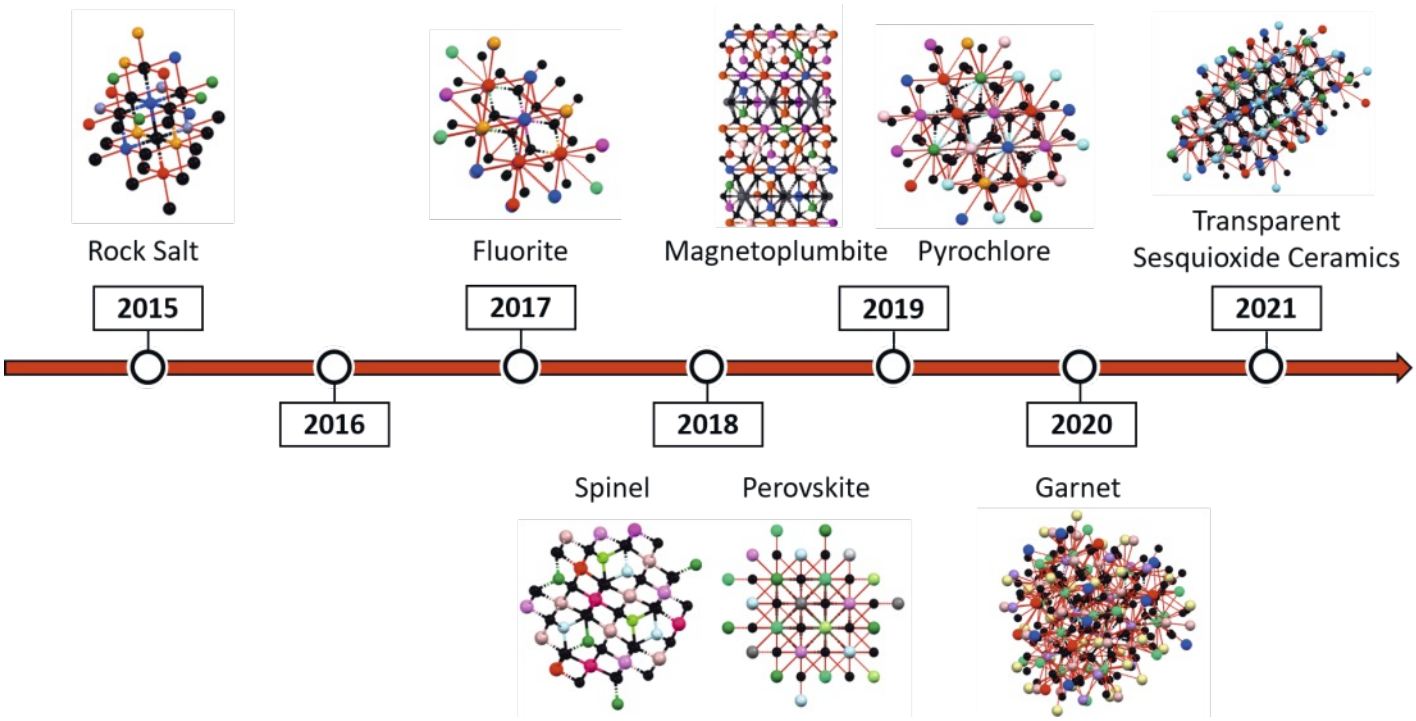

Fig. 2. Timeline of high-entropy oxide structures.

cur spontaneously when $T\Delta S_{mix} > \Delta H_{mix}$, resulting in a negative Gibbs free energy (ΔG_{mix}). The entropy of mixing (ΔS_{mix}) is composed of vibrational and configurational entropy terms, which are related to the distribution of vibrational modes and distribution of atoms in the crystal lattice, respectively. Assuming a minimal vibrational entropy contribution, ΔS_{mix} is maximized by increasing the configurational entropy. In an ideal HEO system, the oxygen sublattice screens the nearest neighbor cation interactions and $\Delta H_{mix} = 0$; however, lattice distortions, induced by differences in electronegativity or atomic size, may result in a small positive enthalpic term, which must be overcome by the entropic term in order to stabilize the single phase. The total configurational entropy of the system is calculated using Eqn. (1):

$$S_{config} = -R\left[\left(\sum_{i=1}^{N} x_i \ln x_i\right)_{cation-site} + \left(\sum_{j=1}^{N} x_j \ln x_j\right)_{anion-site}\right] \quad (1)$$

where N is the number of unique components within the lattice and x_i is the molar concentration of the i^{th} component. However, when only one anion is present, the total configuration entropy of the system is determined by the number (N) and molar concentration (x_i) of the cations, which is shown in Fig. 3. The configurational entropy is maximized when an equimolar composition is present, and at this point the temperature of the multiphase to single phase transition can be lowered no further, which has been demonstrated experimentally by Rost *et al.*[42] In an equimolar composition, increasing N decreases $\Delta H_{mix,}$ and, as a consequence, lower temperatures can drive the multi- to single-phase transition.

With the possibility of a vast number of multi-element compositional configurations, along with the diversity of crystal structures possible, the field of high entropy oxides allows for a plethora of avenues to be explored for the rational design and engineering of tailorable materials relevant to the energy challenges of the future.

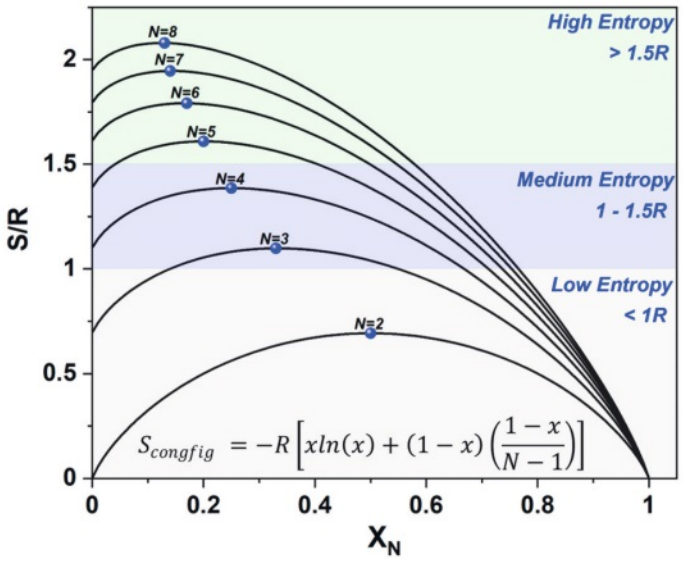

Fig. 3. Configurational entropy change as a function of the number of cations (N) and the cation mole fraction of an N^{th} component (X_N). The maximum entropy is attained at equimolar compositions. Depending on S/R, one distinguishes between low, medium and high entropy materials.

2. Microstructure Control of High-entropy Ceramics

2.1 *Synthesis*

The most widely used and studied synthesis technique for HECs is a solid-state reaction synthesis that intertwines synthesis, shaping, and sintering processes. This often calls for multiple oxide powders with different elemental compositions being ground or mixed together, pressed into a pellet, and followed by reactive sintering heat treatment in order to form a single phase by inter-diffusion and/or reaction.[55–58] However, this process can pose an issue for controlling and tailoring the microstructure. Conversely and especially in the case of oxides, focus has recently been given to synthesis strategies to decouple the syn-

thesis, shaping, and sintering process by first synthesizing HEC powders. The motivation behind such synthesis strategies is to gain control of the crystalline size, morphology, and porosity as well as expand the range of the elemental compositions. A myriad of techniques have been successful for the synthesis of HECs including spray pyrolysis,[59] co-precipitation,[59] hydrothermal,[60] mechano-chemical,[61] sol-gel,[62] solution combustion,[63] and sonochemistry.[64] Below we highlight certain synthesis strategies that may have implications for future microstructure engineering of HECs.

2.1.1 *Current Synthesis Strategies*

Particle Size and Morphology

Nano-sized particles often exhibit different properties than their larger counterparts, and the synthesis of nano-sized HEOs will considerably increase the materials engineering space for HEOs.[65] With respect to ceramics, nano-powders are additionally interesting as particle size of the starting powder directly affects the surface energy and therefore influences the sintering process and the final microstructure.

The first comprehensive study on nano-sized HEOs was by Sarkar *et al*.[59] comparing different synthesis techniques like flame spray pyrolysis (FSP), nebulized spray pyrolysis (NSP), and reverse co-precipitation. From this study, NSP was the most successful in directly synthesizing nanocrystalline HEO powder (with rock-salt structure) while FSP and reverse co-precipitation required an additional calcination step to achieve a single phase. As a follow-up to this initial study, several HEO phases have been synthesized using NSP, specifically fluorite,[48] perovskite,[51] and spinel structures.[66] However, the NSP method results in broad particle size distributions and non-uniform particle shapes.

To achieve narrower size distributions, other wet-chemistry techniques like precipitation[67] and hydrothermal[68] synthesis followed by a subsequent thermal treatment step have been used to produce nano-sized HEOs. Similarly, a modified solution combustion synthesis technique has been shown by Mao *et al.* to synthesize nano-sized HEOs along with additional control of the particle size through the synthesis temperature.[63,69] This work also highlights why such attention should be given to producing uniform morphologies and narrow particle size distribution, because many properties, specifically magnetism in that study, are also affected by particle size.

In addition to particle size, the morphology of the synthesized powder can also influence the final microstructure. Currently, morphological studies of the synthesis of HEO primarily rely on comparing the final resulting powders from different synthesis techniques and different chemistries. Albedwawi *et al.* summarized the current state of the art for different morphologies for rock-salt HEOs[70] where a similar spherical morphology has been observed across many synthesis techniques, though they have not always been uniform with additional cuboidal morphologies being present as well. Additionally the selection of cations may also play a role in the final morphology. In the case of reversed precipitation, the change of the selection of cation (Fe and Mn instead of Mg and Zn) resulted in non-uniform cuboidal instead of spherical particle. However, comprehensive studies along with strategies to synthesize a range of different morphologies remains incomplete.

Low-temperature Synthesis

Most synthesis techniques mentioned above require elevated temperatures for the HEO phase to form, which may limit the range of elements and dopants that can be used. This is especially important for energy storage applications that benefit from incorporation of elements like lithium, which tends to vaporize at higher temperatures. Mechano-chemical techniques, where high energy milling instead of high temperatures is used to mix and form the single HEO, has in such cases proven successful for incorporating lithium and sodium into a rock-salt HEO structure.[61] Though much focus is given to incorporating different elements in the cation position, the mechano-chemical technique was also used to incorporate fluorine in the anion positions,[61] which additionally contributes to increased configurational entropy.

2.1.2 *Remaining Challenges in Synthesis*

Since the field of HEO is relatively new, focus has been primarily given to synthesizing different structures with different chemistries and testing properties rather than process optimization to achieve uniform powders. Therefore, the synthesis of HEO powders with a narrow particle size distribution continues to be a challenge and often the particle size and morphology are not given much attention or are not even reported. Particularly promising though have been wet-chemistry techniques where narrow particle size distributions were achieved. Additionally in traditional ceramic powders, such techniques have been used to synthesize different powder morphologies. However, as observed with reverse precipitation and hydrothermal synthesis for HEOs, precursors need to be synthesized first and then calcined to form HEOs. The synthesis of high-entropy precursors with tailorable morphologies could ultimately provide an opportunity to have HEOs with different morphologies. One such precursor is layered double hydroxides which can be synthesized with a range of morphologies. Recently, layered double hydroxides (LDHs) have been shown to exist as high-entropy material[71] with up to 8 cations incorporated in the structure.[72] Such material could combine the need for tailorable morphologies and multiple cation incorporation in order to explore powder morphology driven microstructure engineering.

2.2 *Sintering Strategies*

In addition to the chemical composition, the particle shape and morphology control during synthesis, the sintering step has a significant effect on the material properties. To fully develop and exploit the potential of HECs, in-depth sintering studies are required, analogous to the decades long research on sintering for low-entropy ceramics.

2.2.1 *Current Strategies*

Reactive sintering of an appropriate mixture of powders as well as sintering of HEC powders is commonly reported in literature.[46,57,58] Though reactive sintering has the benefit of avoiding many HEC powder synthesis-related issues, it limits the range of achievable microstructures. Following the high sintering temperatures or long dwell times required to form phase-pure HECs,[57] extensive grain growth may occur despite the reduced accompanying energy gains, as a result of the increased crystalline energy due to lattice distortions in HECs.[73]

Dense high-entropy ultra-high temperature ceramics (UHTCs) are particularly difficult to achieve.[46,56,74] Reactive flash spark plasma sintering has allowed successful production of high-entropy carbides and borides from the respective constituent metal carbide and boride powders, respectively[56,58] For high entropy borides, addition of carbon can further enhance sintering, allowing for oxides to be efficiently removed.[58] Excess carbon has also been reported beneficial to the sintering of high entropy carbides,[75] supposedly favoring grain boundary diffusion as observed in the case of SiC.[76]

Both conventional[57,75,77] and fast sintering techniques such as flash or spark plasma sintering[46,56,58,78] have been successfully used with both phase-pure HEC powders as well as reactive powder mixtures. Pressure-assisted fast sintering techniques readily allow for the achievement of highly dense and fine microstructures. Microstructural refinement tends to increase a region that some authors refer to as the ‘phase spectrum’; the temperature

range at which the reduced contribution of the entropic term leads to the formation of a multi-phase microstructure.[42,57] This reversible phase change is in contrast to purely segregation-driven secondary phase precipitation in conventional doped ceramics. In the latter, grain growth and dopant segregation are required to accumulate dopants at the grain boundaries and eventually induce dopant-rich second phase precipitation. Indeed, within the phase spectrum, secondary phase generation at the grain boundaries as well as within the grains is observed (Fig. 4).[57] Depending on the grain size, secondary phases are observed at the grain boundaries, within the grains or in the form of entirely transformed grains. The latter occurring only in refined microstructures, it may be suggested that the phase change is dependent on both a probabilistic (*e.g.* nucleation site) and length scale (*e.g.* diffusion length) factor. Since secondary phases are also observed within the grains for the larger case, the increase of the phase spectrum range with fine microstructure refinement is believed to be length-scale driven.

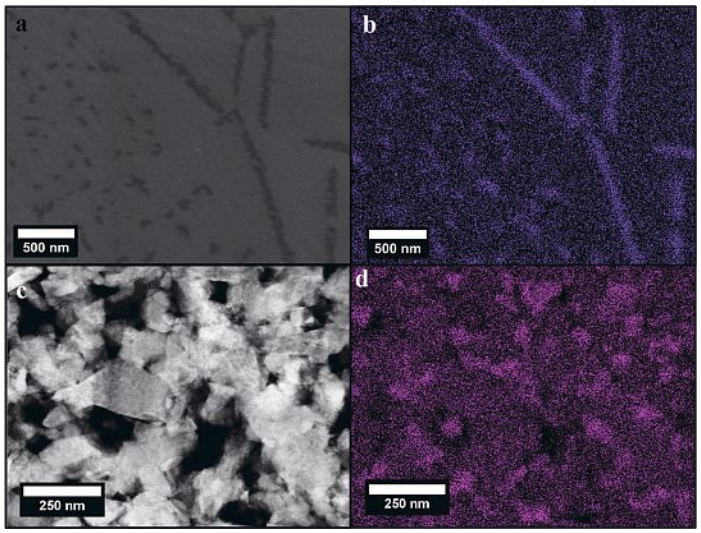

Fig. 4. Morphology of the secondary phase after heat treatment of (Co,Cu,Mg,Ni,Zn)O. (a) SEM micrograph of a 25 mm average grain size sample treated at 700 °C for 12 h and (b) the corresponding EDS map for CU. (c) STEM micrograph of a 89 nm average grain size sample after sequentially heat treating from 450–550 °C in 2 h increments, and (d) the corresponding EDS map for CU. Figure reproduced under CC BY from Dupuy *et al*.[5,7]

Similar to other ceramics, two-step sintering has also been successfully applied to the sintering of HECs as a means to achieve high densities with reduced grain growth,[75,79-81] underscoring the importance of kinetic effects in spite of the lower excess energy associated with the grain boundary interfaces in high entropy ceramics. Since in many cases an excellent high temperature stability has also been reported,[79] more work is required towards microstructure and more specifically grain boundary engineering in HECs. Indeed, little is reported so far on selective doping effects, grain boundary segregation in general, and thus potential complexion transitions in HECs.

2.2.2 *Remaining Challenges and New Frontiers in Sintering and Microstructural Control*

Due to remaining challenges on the synthesis side, microstructure and grain boundary engineering in HECs is still largely unexplored. It requires the study of the interplay between composition, potentially related grain boundary segregation, the phase spectrum, complexion transitions and the sintering conditions. While this may not be as critical for grain boundary-independent material properties, grain boundary-dependent properties rapidly need to be considered under these appropriate factors to evaluate and develop the potential of HEC in numerous technical applications.

Grain boundaries can be considered as interfacial phases that can undergo first order or continuous phase-like transitions that depend on the thermodynamic potentials (T, P, μ) employed. These distinct grain boundary phases are thermodynamically two-dimensional and are known as complexions. Changes in grain boundary complexions can result in sudden changes in grain boundary structure and chemistry, affecting grain boundary properties such as grain growth, creep, mobility, diffusivity, as well as thermal, electronic, and ionic conductivity. A deep understanding of complexion transitions is paramount if HECs, and high-performance ceramics in general, are to be tailored for high-value applications, pertinent to global future energy issues. The grain boundary energy (γ_{gb}) in a multicomponent system is defined by Eqn. (2):

$$\gamma_{gb} = e^{xs} - s^{xs} - \sum_i \mu_i \Gamma_i \qquad (2)$$

where e^{xs} is the excess internal energy, s^{xs} is the excess entropy, μ_i is the chemical potential and Γ_i the adsorption of the i^{th} solute component, respectively. All parameters represent the interfacial excess quantities per unit area. Therefore, the system will tend to minimize γ_{gb} by varying the composition and structure of the interfacial grain boundary region by forming a specific complexion state. Additionally, metastable complexions may form and can be stabilized by grain boundary transitions depending on the value of the thermodynamic potentials. This includes formation of more disordered grain boundary complexions, which are stabilized at high temperature. In multicomponent HEC systems, adsorption of multiple solutes at the grain boundaries may introduce additional grain boundary configurational entropy, which could stabilize metastable complexions and induce novel phenomena at the grain boundaries. Therefore, at high temperature, and through careful control of the thermodynamic potentials *via* the sintering program, this may allow the entropic stabilization of grain boundary metastable states, producing high entropy grain boundary complexions and highly stable interfacial grain boundary regions. This has been observed in HEA, where the thermodynamic driving force for grain growth is suppressed by the formation of high entropy stabilized complexions at high temperature, which reduces the grain boundary energy significantly, as shown in Fig. 5.[82]

Hence, tailoring of the HEC microstructure through control

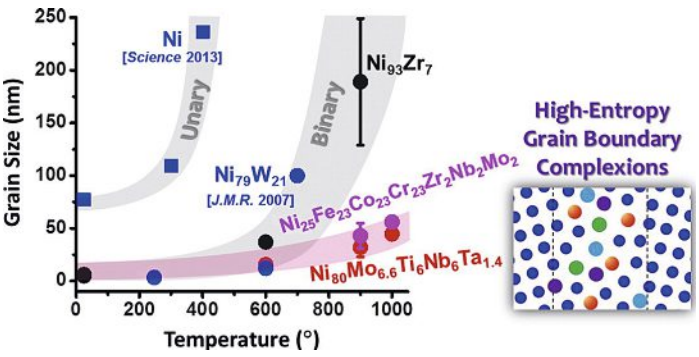

Fig. 5. Grain size vs. annealing temperatures for high-entropy alloys $Ni_{25}Fe_{23}Co_{23}Cr_{23}Zr_2Nb_2Mo_2$ and $Ni_{80}Mo_{6.6}Ti_6Ta_{1.4}$ compared to Ni and binary alloys $Ni_{93}Zr_7$, $Ni_{79}W_{21}$. Reprinted with permission from Zhou *et al*., *Scripta Mater*. **2016**, *124*, 160.[82] Copyright 2016 Elsevier.

and formation of high entropy stabilized grain boundary complexions could result in novel and unprecedented grain boundary phenomena. Therefore, characterization of complexion transitions, and of grain boundary types and population distribution, is of utmost importance.

2.3 *Current Status of Microstructure Analysis and Chemical Signatures of Entropic Stabilization*

In order to make advancements in the rational design of functional HECs, and advanced functional materials in general, the intimate relationships between complexion transitions, grain boundary structure and chemistry, and the resulting functional properties must be elucidated in detail. Cutting-edge techniques for identifying the signatures, both directly and indirectly, of complexion transitions are currently being developed. High-throughput techniques, such as scanning electron microscopy-electron backscattered diffraction, combined with stereological analysis provide indirect evidence of complexion transitions, as well as characterization of the grain boundary character distribution, as shown in Fig. 6.[83]

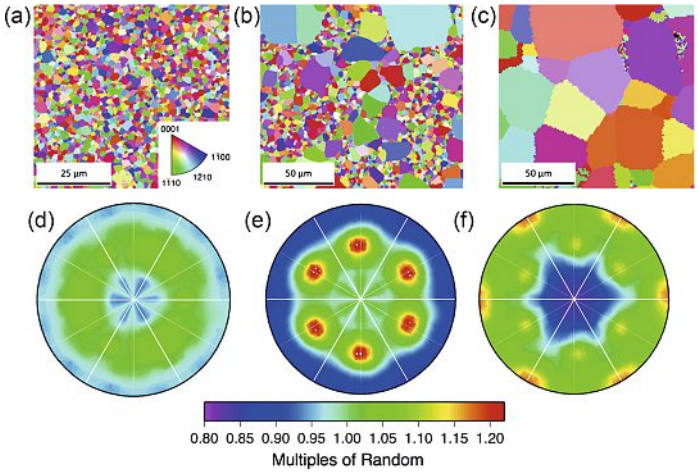

Fig. 6. Orientation maps illustrating the [(a)–(c)] microstructures and [(d)–(f)] grain boundary plane distributions for 450 ppm Y-doped alumina, sintered at [(a) and (d)] 1450 °C, [(b) and (e)] 1500 °C and [(c) and (f)] 1600 °C. The grain boundary plane distributions are plotted in stereographic projection with the [0001] direction normal to the page and the [11$\bar{2}$0] reaction horizontal. Reprinted with permission from Rohrer, *Curr. Opin. Solid St. Mater*. **2016**, *20*, 231.[83] Copyright 2016 Elsevier.

In terms of identifying whether a HEC is truly entropically stabilized, several complementary techniques are typically used. Entropic stabilization requires the presence of a reversible solid-state multi- to single-phase transformation, with the single phase exhibiting a random and homogenous distribution of cations within the sublattice. Reversibility can be assessed by monitoring the transition from multi-phase to single-phase, as a function of temperature, using X-ray diffraction. If the system is truly entropically stabilized, then entropy is maximized at an equimolar cation composition, and the multi-phase to single-phase transition temperature cannot be lowered further. Therefore, signatures of entropic stabilization can be identified by varying the mole fraction of the n^{th} component in the region of the equimolar composition, which will cause the phase transformation temperature to increase. True entropic stabilization also requires that the positive enthalpic term be compensated by the entropy term; therefore, endothermicity is a prerequisite for true entropic stabilization. This can be identified using differential scanning calorimetry (DSC), combined with *in situ* temperature-dependent XRD. Hence, the phase transition and heat flow into the sample should occur contemporaneously for an entropically stabilized process. Finally, the random and homogenous distribution of cations within the sublattice can be investigated by extended X-ray absorption fine structure (EXAFS), which should show oscillations with similar relative intensity and reciprocal spacing for each incorporated cation within the lattice, as shown in Fig. 7.[42]

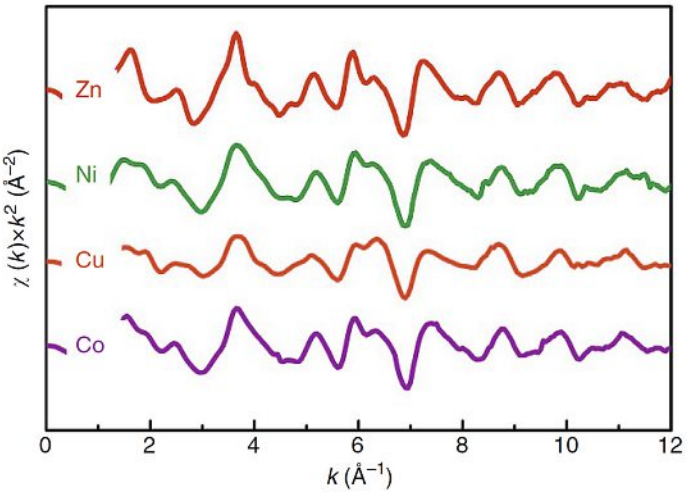

Fig. 7. EXAFS measured at Advanced Proton Source beamline 12-BM after energy normalization and fitting. It can be observed that the oscillations for each element occur with similar relative intensity and at similar reciprocal spacing. This suggests a similar local structural and chemical environment for each of the elements. Figure reproduced under license CC BY from Rost *et al*.[42]

3. Applications

Synergistic, or cocktail effects, entropic stabilization and slow kinetic phenomena present in HECs yield additional degrees of freedom for the design of advanced materials for multifunctional devices. HECs can enhance mechanical, thermal, catalytic, electrical, optical and magnetic properties, as well as improved ionic conductivity, biocompatibility, and oxidation and corrosion resistance compared to their low-entropy analogues. Some recent advancements in applications are highlighted in this section.

3.1 *Catalysis*

Thermal catalysis, using supported metal catalysts, is pivotal for the chemical, environmental and automotive industries. Surviving the harsh operating conditions and maintaining catalytic performance is essential for these sectors. For processes such as steam reforming, exhaust treatment and catalytic combustion, high temperature operation results in migration and sintering of homogenously distributed noble metal catalyst particles, such as Pt and Pd, which dramatically reduces active surface areas, resulting in diminishing catalytic performance. Therefore, high temperature stability is crucial in order to improve catalytic process lifetimes. In the context of HECs, one of the most widely studied catalytic reactions thus far is the oxidation of CO. Entropy-stabilized metal oxides have recently demonstrated improved CO oxidation high-temperature stability,[84] while also requiring lower amounts or even suppressing the need of the noble metal catalyst.[85] These high entropy oxides can perform conversions at lower temperatures compared to their conventional metal oxide analogues,[70] as well as stabilize the noble metal, which in return reduces the degree of sintering, improves dispersion and increases catalyst lifetimes.[84] These observations are attributed to synergistic 'cocktail' effects, as well as enhanced surface acidity/basicity and oxygen mobility, due to the facile formation and tunability of oxygen vacancies.[70] Similar findings have also been reported for CO_2 hydrogenation,[86] CH_4 partial oxidation,[87]

alcohol oxidation[88] and oxidative desulphurization.[89] With a tolerance of the crystal structure towards high temperatures and chemical environments, high-entropy ceramics, including LDHs, are more chemically stable and can maintain either their crystal structure or porous structure in certain catalyst-toxic atmospheres. It is reported that a superior sulphur tolerance has been observed in some mesoporous samples.[90] In the high-entropy system, a new parametric space is added, allowing the tailoring of material properties *via* small changes in their constituents. Thus, material surface area and porosity are significant factors in catalysis and may be easier to modify and enhance compared with the ordinary, low entropy materials to improve the catalysis performance.

From a microstructural engineering perspective, materials such as MgO exhibit high concentrations of Lewis basic sites at grain boundaries due to the formation of disordered atomic layers. These layers contain low coordinated O^{2-} ions that result in additional electronic states in the band gap close to the bottom of the conduction band. This results in significant electron delocalization in the region around the O^{2-} ions situated along the grain boundaries. Consequently, increased adsorption energies for target gas molecules can result, which can facilitate dissociative adsorption of adsorbate molecules. This has been calculated using DFT analysis for CO_2 adsorption on MgO, where the O=C=O bond angle decreases from 178° on regular surface O ion sites to 161° for grain boundary O ion sites, as shown in Fig. 8A.[91,92] The deformation of the CO_2 molecule at site 1 is due to increased total electron density in the bridging region and an enhanced dipole-induced interaction, as shown in Fig. 8B.[91] Consequently, the grain boundary regions of HEOs may provide high adsorption energies for molecules such as CO_2. A thorough analysis of the interplay between complexion transitions, grain boundary chemistry and structure could result in a paradigm shift, resulting in the generation of grain boundary engineered high entropy catalysts. As a result, high-entropy ceramics could lead to promising new avenues and applications for thermally activated-, photo-,[70] and electro-[93] catalytic-based processes.

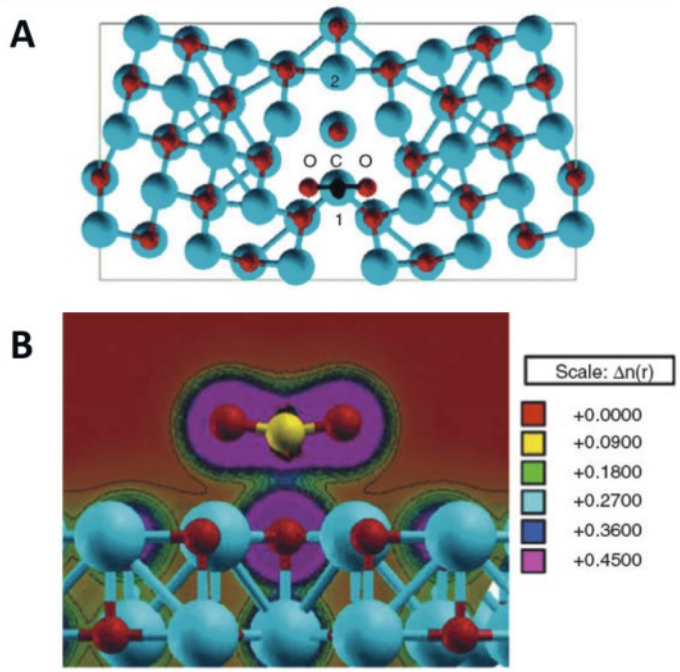

Fig. 8. (A) Top view of the MgO supercell showing the adsorption of CO_2 on a grain boundary oxygen ion site (marked at 1 and 2). (B) Electron density distribution map of CO_2 absorped on site 1. Reprinted with permission from Landau *et al*., *Rev. Chem. Eng.* **2014**, *30*, 379.[91] Copyright 2014 Walter de Gruyter GmbH.

3.2 *Energy Storage: Batteries and Capacitors*

For electrochemical energy storage, intercalation-based Li-ion batteries offer a promising energy storage capacity, combined with high efficiency and reversibility.[94,95] Indeed, for high and reversible Li-ion storage capacity, the host crystal structure needs to provide two (usually) conflicting properties: high density of Li-storage space and high crystal structure stability. Here HECs are promising candidate materials overcoming the inherent discrepancy. Indeed, the intrinsic configurational disorder leads to the stabilization of crystal structure. Thus, high-entropy oxides show a more stable specific capacity even after hundreds of cycles,[96] compared with their medium-entropy counterparts (Fig. 3). In addition, and similar to HEAs, considerable lattice distortion in HECs affects the diffusion kinetics as well as the mechanical properties, able to reduce or eliminate problems linked to particle aggregation and cracking during the charge-discharge cycles.[97,98] Thus, HEC anodes tend to display better structural stability and robustness.[99] However, the ion mobility is also a critical parameter which has to be considered for promising ion-battery materials. High lithium and sodium ion mobilities have been reported for instance in $(MgCoNiCuZn)_{1-x-y}Ga_yA_xO$ (with A = Li or Na).[96] Observed Li^+ ion conductivities were able to exceed 10^{-3} S cm^{-1} at room temperature, surpassing the values observed in LiPON, a longtime reference, by two orders of magnitude. Following this observation, it has been suggested that this high ion conductivity was linked to large amounts of alkali elements in the host lattice. Indeed, when their concentration increases, the density of oxygen vacancies increases as well, which can percolate to form diffusion channels. The existence of such diffusion channels also lowers the diffusion activation energies, speeding up the cation diffusion and ion mobility.[100]

The storage capacity can furthermore be tuned through a wide field of possible chemical compositions, affecting the lattice deformation and thus the volume of interstitial sites. It illustrates how HECs offer new ways to engineer the storage capacity while preserving a high crystal stability, required for stable cycling performance.

In addition to ion batteries, electrochemical capacitors – also known as supercapacitors – play a significant role for energy storage required to successfully implements societal energy transition efforts. This is due to their high power density and 'unlimited' charge–discharge cycle life (>10^6 cycles), core properties evaluated in the quest for promising future electrochemical capacitor materials. Indeed, Bérardan *et al.* reported that certain rock-salt HEOs exhibit colossal dielectric constants, paving the way towards capacitors with extra-large energy densities.[101,102] High-entropy nitrides have also shown promise, with a competitive specific capacitance of 78 F g^{-1} achieved at a scan rate of 100 mV s^{-1} in 1 M KOH.[103] Following these observations and given the 'intrinsic' advantage of tailorable electron states and crystal stability, HECs have attracted attention in the research community. Potential applications are numerous in modern microelectronics and new capacitance-based energy storage devices.

3.3 *Energy Harvesting: Thermoelectrics*

Oxide ceramics are considered as promising thermoelectric (TE) materials[104,105] for high temperature applications because of their high chemical and thermal resistance, low processing cost, as well as environmental friendliness. The thermoelectric performance of TE materials is commonly evaluated considering a dimensionless figure of merit (Eqn. (3)):[106]

$$ZT = \frac{S^2\sigma}{\kappa_t} \qquad (3)$$

where *S* is the Seebeck coefficient, describing the electron potential difference in the sample when subjected to a temperature gradient, σ corresponds to the electrical conductivity, and κ_t is the thermal conductivity. The thermal conductivity, κ_t, is usually the sum of two possible heat transport mechanisms: (a) electron-hole (κ_e), and (b) phonon (κ_l) diffusion:

$$\kappa_t = \kappa_e + \kappa_l \quad (4)$$

To increase the figure of merit, *ZT,* the thermal conductivity of the material should be minimized. This can be achieved by reducing the phonon transport (κ_l) in the material. Indeed, κ_l depends on phonon scattering within the crystal lattice, which can be promoted by disorder in the crystal structure. Thus, doping with heavy metals, complexification or deformation of the crystal structure, refining of the microstructure, modification of the grain boundary structure and finally amorphization of the crystal are efficient methods to reduce the thermal conductivity. Following this concept, the TE study of complex structured materials can often be performed following the phonon glass–electron crystal (PGEC) paradigm:[107] a complex crystal structure can be regarded as a phonon glass and/or an electron crystal governing the *ZT* values of TE materials.

The interest in metal oxide-based TE materials results from their extremely low κ_l values, which can be modified by selective doping and microstructure engineering.[108,109] Moving from low-entropy to high-entropy ceramics therefore opens a new parametric space, allowing for tailored material properties *via* compositional changes. Indeed, it allows modifying the lattice distortion over a wide range and gives the opportunity to explore cocktail effects, promoting phonon scattering and thereby lowering κ_l. This has been confirmed in a study on a $SrTiO_3$-based high-entropy perovskite, which has led to a thermal conductivity as low as 0.7 W/mK at 1100 K.[110] In addition to these compositional effects, selective doping and/or the sintering strategy may further modify the properties *via* the grain boundary structure and character distribution. In combination with HECs, gaining new insight into microstructure engineering may thus enable further fine tuning of the material, underscoring the potential of high-entropy ceramics to develop and engineer high *ZT* materials for the future.

3.4 *Energy Transport: Superconductors and Sensors*

Some crystal structures such as high-entropy layered double hydroxides (HE-LDHs) are characterized by quasi-two-dimensional layers formed by octahedrally coordinated metal cations, which may serve as a basis to realize a 2-D electron gas and high-temperature superconductivity.[71] For HE-LDHs, the crystal structure and cation coordination shows similarities to the one of superconducting cuprates.[111] Through changes of their chemical composition, the crystal structure and lattice parameters can be adjusted to further approach those of superconductor cuprates. Profiting from the random and homogeneous distribution of multiple cations, it is possible to adjust the valence states of cations on long- and/or short-range orders. Consequently, it is possible to tune their cation electron states to get close to a $3d^{9\pm\delta}$ state at which cuprates can exhibit superconductivity.[112]

We have synthesized a set of HE-LDHs, precursors to layered HECs, in which we inserted mostly cations of third-period transition metals that show different magnetic properties. It should therefore be possible to demonstrate an antiferromagnetic state – the ground state of superconductor cuprates – by adjusting the electron states and/or lattice parameters through modification and fine-tuning of its constituent elements.[112] This should offer the possibility to reach a short-range magnetic behavior by tweaking the electronic state through compositional changes, thereby opening the path towards superconducting states. Indeed, short-range magnetic phenomena such as a spin-glass behavior, with several possible magnetic phase transitions, could already be observed in some of our $[M_{1-x}^{2+}M^{3+}(OH)_2]A_{x/n}^{n} \cdot mH_2O$ (M represents Mg^{2+}, Ni^{2+}, Cu^{2+}, Co^{2+}, Zn^{2+}, Al^{3+}, Cr^{3+}, and Fe^{3+} and A represents an n-valent anion) HE-LDH samples (Fig. 9). This finding may provide guidance towards the corroboration of superconductor traces in this material. HE-LDHs, and potentially some layered HECs, may thus have the potential to express superconductivity, and if so become a superconductor family to be explored in the quest for viable high-temperature superconductivity solutions.

With a space group *R-3m* crystal structure, (HE-)LDHs are anisotropic: the metal-oxide octahedra are distorted being either elongated or compressed. Following their different outer shell *d*-electrons, transition-metal ions are particularly sensitive to distortion. Indeed, the rearrangement of *d*-electrons under the influence of the crystal field is always observed. This rearrangement, known as the Jahn-Teller effect, can lead to degeneration of the *d*-electrons, giving rise to the formation of anisotropic *d*-orbitals. This, in turn, may lead to interesting electronic and magnetic material behaviors. Because the lattice parameters are a function of the temperature, the electronic and/or magnetic properties will change with temperature as well. For this reason, it is possible that at a certain temperature, the energy of the crystal field reaches a critical level at which rearrangement of *d*-electrons occurs, which can be detected as anomalies in the electronic and/or magnetic behavior. Materials expressing such anomalies can also serve as sensors for specific applications.[113,114] Since for HE-LDHs, and other HECs, the crystal structure can be tuned to a large extent and the composition changed, the crystal field, the associated critical temperature as well as the intensity of the anomaly may be tuned for specific needs.

4. Contemporary Challenges and Future Perspectives

High-temperature entropic stabilization of a ceramic single phase from multiphase composition can be achieved by exploring a vast parameter space, including a diverse range of crystal structures, cations and cation properties. A thorough understanding of composition–structure–property relationships may allow tailoring of HECs to specific high-value applications. One major challenge lies in understanding and predicting the complex interplay between configurational entropy, mixing enthalpy, cation size, coordination number and oxidation state on the resulting functional properties. For instance, tailoring of elements with different valence states could lead to specific catalytic and adsorption properties, due to subtle changes in charge compensation mechanisms. From a microstructural perspective, understanding the relationships between powder processing and synthesis routes on the bulk and grain boundary characteristics is another key challenge, not only for HEC but also for high performance ceramics in general. Additionally, many other parameters could contribute to configurational entropy stabilization. This was highlighted by Djendadic *et al.* regarding the subtle role of rare-earth elements on entropic stabilization of the single phase.[48] Elucidating these complex interrelationships will require a combination of experimental and theoretical computational methods, such as DFT, MC+MD and CALPHAD – with associated challenges in combination with HECs – in order to generate HEC design pipelines. Practically speaking, another major challenge for commercialization will be the development of synthesis and sintering methods for industrial scale-up. Overall, the potential of HEC materials to surmount current and future energy related issues is extremely promising. The next challenge will be to understand and harness their unique characteristics as effectively as possible.

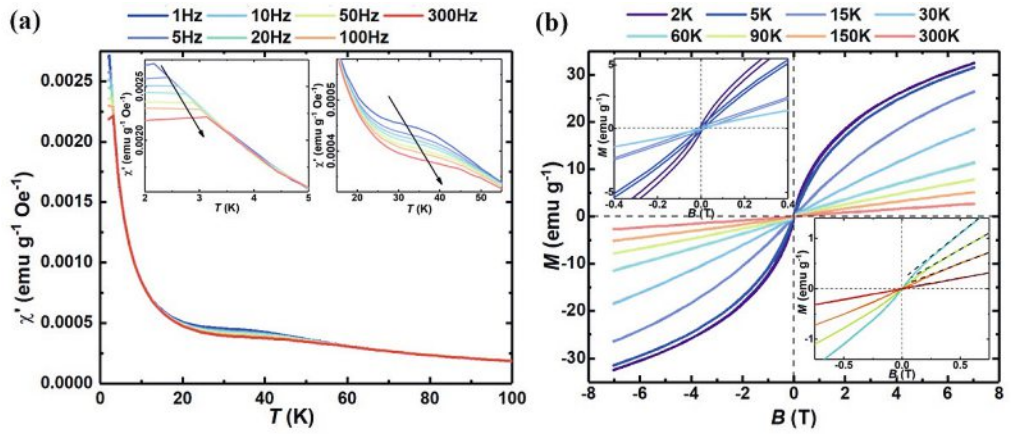

Fig. 9. (a) Real part (χ') of the AC susceptability for an $[M_{1-x}^{2+}M^{3+}(OH)_2]A_{x/n}^{n}\cdot mH_2O$ (M represents Mg^{2+}, Ni^{2+}, Co^{2+}, Zn^{2+}, Al^{3+}, Cr^{3+}, and Fe^{3+} and A represents an n-valent anion). LDH sample as a function of temperature and frequency from 2 to 300 Hz, and the inserts are in an expanded scale to show the AC frequency dependence. (b) Isotherm magnetization *M(H)* loops of the LDH sample with magnetic fields ranging from –7 to 7 T at temperatures between 2 and 300 K; the top-left is in an expanded scale to show the hysteretic behavior at low temperatures, and the dash lines in the bottom right give a guide to show the linear behavior at high temperature.

5. Conclusions

High-entropy stabilized materials, which contain five or more cations, exhibit properties that are not typically observed in low entropy analogues. These properties are a result of several combined structural and chemical characteristics, including synergistic 'cocktail' effects, arising due to the random distribution of several metal cations; sluggish diffusion kinetics; entropic stabilization and lattice distortion. These inherent qualities result in materials with enhanced thermal, electronic, and ionic conductivities, as well as optical, catalytic and mechanical properties. Research on HECs is rapidly gaining momentum, with the current focus mainly on oxide materials, although research on hydrides, carbides, nitrides, sulphides, silicides, fluorides, including others, is also increasing rapidly. In summary, these materials offer exciting new prospects in order to overcome tomorrow's global energy and environmental challenges.

Received: December 14, 2021

[1] R. Apetz, M. P. B. van Bruggen, *J. Am. Ceram. Soc*. **2003**, *86*, 480, https://doi.org/10.1111/j.1151-2916.2003.tb03325.x.

[2] A. Krell, P. Blank, H. W. Ma, T. Hutzler, M. P. B. van Bruggen, R. Apetz, *J. Am. Ceram. Soc*. **2003**, *86*, 12, https://doi.org/10.1111/j.1151-2916.2003.tb03270.x.

[3] J. P. Cheng, D. Agrawal, Y. J. Zhang, R. Roy, *Mater. Lett*. **2002**, *56*, 587, https://doi.org/10.1016/S0167-577x(02)00557-8.

[4] O. H. Kwon, C. S. Nordahl, G. L. Messing, *J. Am. Ceram. Soc*. **1995**, *78*, 491, https://doi.org/10.1111/j.1151-2916.1995.tb08829.x.

[5] C. Pecharroman, G. Mata-Osoro, L. A. Diaz, R. Torrecillas, J. S. Moya, *Opt. Express* **2009**, *17*, 6899, https://doi.org/10.1364/Oe.17.006899.

[6] J. G. J. Peelen, R. Metselaar, *J. Appl. Phys*. **1974**, *45*, 216, https://doi.org/10.1063/1.1662961.

[7] D. Carloni, G. Zhang, Y. Wu, *J. Eur. Ceram. Soc*. **2021**, *41*, 781, https://doi.org/10.1016/j.jeurceramsoc.2020.07.051.

[8] Y. Sun, M. Li, Y. L. Jiang, B. H. Xing, M. H. Shen, C. R. Cao, C. Wang, Z. Zhao, *Adv. Eng. Mater*. **2021**, *23*, https://doi.org/10.1002/adem.202001475.

[9] A. P. Schlup, W. J. Costakis, W. Rheinheimer, R. W. Trice, J. P. Youngblood, *J. Am. Ceram. Soc*. **2020**, *103*, 2587, https://doi.org/10.1111/jace.16932.

[10] A. Dash, B. N. Kim, J. Klimke, J. Vleugels, *J. Eur. Ceram. Soc*. **2019**, *39*, 1428, https://doi.org/10.1016/j.jeurceramsoc.2018.12.004.

[11] M. Trunec, J. Klimke, Z. J. Shen, *J. Eur. Ceram. Soc*. **2016**, *36*, 4333, https://doi.org/10.1016/j.jeurceramsoc.2016.06.004.

[12] M. Stuer, P. Bowen, *Adv. Eng. Mater*. **2014**, *16*, 774, https://doi.org/10.1002/adem.201400099.

[13] M. Stuer, Z. Zhao, U. Aschauer, P. Bowen, *J. Eur. Ceram. Soc*. **2010**, *30*, 1335, https://doi.org/10.1016/j.jeurceramsoc.2009.12.001.

[14] A. Krell, T. Hutzler, J. Klimke, A. Potthoff, *J. Am. Ceram. Soc*. **2010**, *93*, 2656, https://doi.org/10.1111/j.1551-2916.2010.03814.x.

[15] P. R. Cantwell, T. Frolov, T. J. Rupert, A. R. Krause, C. J. Marvel, G. S. Rohrer, J. M. Rickman, M. P. Harmer, *Annu. Rev. Mater. Res*. **2020**, *50*, 465, https://doi.org/10.1146/annurev-matsci-081619-114055.

[16] M. P. Harmer, G. S. Rohrer, *Curr. Opin. Solid St. M*. **2016**, *20*, iv, https://doi.org/10.1016/S1359-0286(16)30168-1.

[17] G. S. Rohrer, D. M. Saylor, B. El Dasher, B. L. Adams, A. D. Rollett, P. Wynblatt, *Z. Metallkd*. **2004**, *95*, 197, https://doi.org/10.3139/146.017934.

[18] J. G. Bell, T. Graule, M. Stuer, *Appl. Phys. Rev*. **2021**, *8*, https://doi.org/10.1063/5.0048697.

[19] F. S. Shiau, T. T. Fang, T. H. Leu, *Mater. Chem. Phys*. **1998**, *57*, 33, https://doi.org/10.1016/S0254-0584(98)00195-3.

[20] A. Krell, J. Klimke, *J. Am. Ceram. Soc*. **2006**, *89*, 1985, https://doi.org/10.1111/j.1551-2916.2006.00985.x.

[21] Y. Sakka, T. S. Suzuki, *J. Ceram. Soc. Jpn* **2005**, *113*, 26, https://doi.org/10.2109/jcersj.113.26.

[22] Y. Sakka, T. S. Suzuki, K. Kitazawa, *Euro Ceramics Vii, Pt 1-3* **2002**, *206-2*, 349, https://doi.org/10.4028/www.scientific.net/KEM.206-213.349.

[23] A. D. Moriana, S. J. Zhang, *J. Materiomics* **2018**, *4*, 277, https://doi.org/10.1016/j.jmat.2018.09.006.

[24] S. A. Bojarski, M. Stuer, Z. Zhao, P. Bowen, G. S. Rohrer, *J. Am. Ceram. Soc*. **2014**, *97*, 622, https://doi.org/10.1111/jace.12669.

[25] A. R. Krause, P. R. Cantwell, C. J. Marvel, C. Compson, J. M. Rickman, M. P. Harmer, *J. Am. Ceram. Soc*. **2019**, *102*, 778, https://doi.org/10.1111/jace.16045.

[26] X. H. Wang, P. L. Chen, I. W. Chen, *J. Am. Ceram Soc.* **2006**, *89*, 431, https://doi.org/10.1111/j.1551-2916.2005.00763.x.

[27] X. H. Wang, X. Y. Deng, H. L. Bai, H. Zhou, W. G. Qu, L. T. Li, I. W. Chen, *J. Am. Ceram. Soc*. **2006**, *89*, 438, https://doi.org/10.1111/j.1551-2916.2005.00728.x.

[28] F. J. T. Lin, L. C. DeJonghe, *J. Am. Ceram. Soc*. **1997**, *80*, 2269, https://doi.org/10.1111/j.1151-2916.1997.tb03117.x.

[29] S. J. Dillon, M. P. Harmer, *J. Am. Ceram. Soc*. **2007**, *90*, 996, https://doi.org/10.1111/j.1551-2916.2007.01512.x.

[30] S. Galmarini, U. Aschauer, A. Tewari, Y. Aman, C. Van Gestel, P. Bowen, *J. Eur. Ceram. Soc*. **2011**, *31*, 2839, https://doi.org/10.1016/j.jeurceramsoc.2011.07.010.

[31] S. Galmarini, U. Aschauer, P. Bowen, S. C. Parker, *J. Am. Ceram. Soc.* **2008**, *91*, 3643, https://doi.org/10.1111/j.1551-2916.2008.02619.x.

[32] M. T. Buscaglia, V. Buscaglia, M. Viviani, P. Nanni, *J. Am. Ceram. Soc.* **2001**, *84*, 376, https://doi.org/10.1111/j.1151-2916.2001.tb00665.x.

[33] H. Yoshida, S. Hashimoto, T. Yamamoto, *Acta Mater.* **2005**, *53*, 433, https://doi.org/10.1016/j.actamat.2004.09.038.

[34] G. Bernard-Granger, C. Guizard, *Scripta Mater.* **2007**, *56*, 983, https://doi.org/10.1016/j.scriptamat.2007.01.047.

[35] J. Y. Nie, C. Z. Hu, Q. Z. Yan, J. Luo, *Nat. Commun*. **2021**, *12*, https://doi.org/10.1038/s41467-021-22669-0.

[36] S. J. Dillon, M. P. Harmer, *J. Am. Ceram. Soc.* **2008**, *91*, 2314, https://doi.org/10.1111/j.1551-2916.2008.02432.x.

[37] S. J. Dillon, M. P. Harmer, *J. Am. Ceram. Soc.* **2008**, *91*, 2304, https://doi.org/10.1111/j.1551-2916.2008.02454.x.

[38] S. J. Dillon, M. Tang, W. C. Carter, M. P. Harmer, *Acta Mater*. **2007**, *55*, 6208, https://doi.org/10.1016/j.actamat.2007.07.029.

[39] O. Schumacher, C. J. Marvel, M. N. Kelly, P. R. Cantwell, R. P. Vinci, J. M. Rickman, G. S. Rohrer, M. P. Harmer, *Curr.*

Opin. Solid St. M. **2016**, *20*, 316, https://doi.org/10.1016/j.cossms.2016.05.004.
[40] K. De Keukeleere, S. Coucke, E. De Canck, P. Van Der Voort, F. Delpech, Y. Coppel, Z. Hens, I. Van Driessche, J. S. Owen, J. De Roo, *Chem. Mater.* **2017**, *29*, 10233, https://doi.org/10.1021/acs.chemmater.7b04580.
[41] J. De Roo, I. Van Driessche, J. C. Martins, Z. Hens, *Nat. Mater*. **2016**, *15*, 517, https://doi.org/10.1038/Nmat4554.
[42] C. M. Rost, E. Sachet, T. Borman, A. Moballegh, E. C. Dickey, D. Hou, J. L. Jones, S. Curtarolo, J. P. Maria, *Nat. Commun*. **2015**, *6*, https://doi.org/10.1038/ncomms9485.
[43] B. Cantor, I. T. H. Chang, P. Knight, A. J. B. Vincent, *Mat. Sci. Eng. a-Struct*. **2004**, *375*, 213, https://doi.org/10.1016/j.msea.2003.10.257.
[44] J. W. Yeh, S. K. Chen, S. J. Lin, J. Y. Gan, T. S. Chin, T. T. Shun, C. H. Tsau, S. Y. Chang, *Adv. Eng. Mater*. **2004**, *6*, 299, https://doi.org/10.1002/adem.200300567.
[45] P. Sarker, T. Harrington, C. Toher, C. Oses, M. Samiee, J. P. Maria, D. W. Brenner, K. S. Vecchio, S. Curtarolo, *Nat. Commun*. **2018**, *9*, https://doi.org/10.1038/s41467-018-07160-7.
[46] J. Gild, Y. Zhang, T. Harrington, S. Jiang, T. Hu, M. C. Quinn, W. M. Mellor, N. Zhou, K. Vecchio, J. Luo, *Sci. Rep. UK* **2016**, *6*, https://doi.org/10.1038/srep37946.
[47] J. Gild, J. Braun, K. Kaufmann, E. Marin, T. Harrington, P. Hopkins, K. Vecchio, J. Luo, *J. Materiomics* **2019**, *5*, 337, https://doi.org/10.1016/j.jmat.2019.03.002.
[48] R. Djenadic, A. Sarkar, O. Clemens, C. Loho, M. Botros, V. S. K. Chakravadhanula, C. Kubel, S. S. Bhattacharya, A. S. Gandhif, H. Hahn, *Mater. Res. Lett*. **2017**, *5*, 102, https://doi.org/10.1080/21663831.2016.1220433.
[49] J. Dabrowa, M. Stygar, A. Mikula, A. Knapik, K. Mroczka, W. Tejchman, M. Danielewski, M. Martin, *Mater. Lett*. **2018**, *216*, 32, https://doi.org/10.1016/j.matlet.2017.12.148.
[50] S. C. Jiang, T. Hu, J. Gild, N. X. Zhou, J. Y. Nie, M. D. Qin, T. Harrington, K. Vecchio, J. Luo, *Scripta Mater*. **2018**, *142*, 116, https://doi.org/10.1016/j.scriptamat.2017.08.040.
[51] A. Sarkar, R. Djenadic, D. Wang, C. Hein, R. Kautenburger, O. Clemens, H. Hahn, *J. Eur. Ceram. Soc*. **2018**, *38*, 2318, https://doi.org/10.1016/j.jeurceramsoc.2017.12.058.
[52] D. A. Vinnik, E. A. Trofimov, V. E. Zhivulin, O. V. Zaitseva, S. A. Gudkova, A. Y. Starikov, D. A. Zherebtsov, A. A. Kirsanova, M. Hassner, R. Niewa, *Ceram. Int*. **2019**, *45*, 12942, https://doi.org/10.1016/j.ceramint.2019.03.221.
[53] Z. F. Zhao, H. M. Xiang, F. Z. Dai, Z. J. Peng, Y. C. Zhou, *J. Mater. Sci. Technol*. **2019**, *35*, 2647, https://doi.org/10.1016/j.jmst.2019.05.054.
[54] H. Chen, Z. F. Zhao, H. M. Xiang, F. Z. Dai, W. Xu, K. Sun, J. C. Liu, Y. C. Zhou, *J. Mater. Sci. Technol*. **2020**, *48*, 57, https://doi.org/10.1016/j.jmst.2020.01.056.
[55] G. R. Zhang, I. Milisavljevic, E. Zych, Y. Q. Wu, *Scripta Mater*. **2020**, *186*, 19, https://doi.org/10.1016/j.scriptamat.2020.04.011.
[56] G. Tallarita, R. Licheri, S. Garroni, R. Orru, G. Cao, *Scripta Mater*. **2019**, *158*, 100, https://doi.org/10.1016/j.scriptamat.2018.08.039.
[57] A. D. Dupuy, X. Wang, J. M. Schoenung, *Mater. Res. Lett*. **2019**, *7*, 60, https://doi.org/10.1080/21663831.2018.1554605.
[58] J. Gild, K. Kaufmann, K. Vecchio, J. Luo, *Scripta Mater*. **2019**, *170*, 106, https://doi.org/10.1016/j.scriptamat.2019.05.039.
[59] A. Sarkar, R. Djenadic, N. J. Usharani, K. P. Sanghvi, V. S. K. Chakravadhanula, A. S. Gandhi, H. Hahn, S. S. Bhattacharya, *J. Eur. Ceram. Soc*. **2017**, *37*, 747, https://doi.org/10.1016/j.jeurceramsoc.2016.09.018.
[60] L. Spiridigliozzi, C. Ferone, R. Cioffi, G. Accardo, D. Frattini, G. Dell'Agli, *Materials* **2020**, *13*, https://doi.org/10.3390/ma13030558.
[61] Q. S. Wang, A. Sarkar, D. Wang, L. Velasco, R. Azmi, S. S. Bhattacharya, T. Bergfeldt, A. Duvel, P. Heitjans, T. Brezesinski, H. Hahn, B. Breitung, *Energ. Environ. Sci*. **2019**, *12*, https://doi.org/10.1039/c9ee00368a.
[62] G. Wang, J. Qin, Y. Y. Feng, B. X. Feng, S. J. Yang, Z. Wang, Y. X. Zhao, J. Wei, *Acs Appl. Mater. Inter*. **2020**, *12*, 45155, https://doi.org/10.1021/acsami.0c11899.
[63] A. Q. Mao, F. Quan, H. Z. Xiang, Z. G. Zhang, K. Kuramoto, A. L. Xia, *J. Mol. Struct*. **2019**, *1194*, 11, https://doi.org/10.1016/j.molstruc.2019.05.073.
[64] F. Okejiri, Z. H. Zhang, J. X. Liu, M. M. Liu, S. Z. Yang, S. Dai, *ChemSusChem* **2020**, *13*, 111, https://doi.org/10.1002/cssc.201902705.
[65] S. J. McCormack, A. Navrotsky, *Acta Mater*. **2021**, *202*, 1, https://doi.org/10.1016/j.actamat.2020.10.043.
[66] A. H. Phakatkar, M. T. Saray, M. G. Rasul, L. V. Sorokina, T. G. Ritter, T. Shokuhfar, R. Shahbazian-Yassar, *Langmuir* **2021**, *37*, 9059, https://doi.org/10.1021/acs.langmuir.1c01105.
[67] M. Biesuz, L. Spiridigliozzi, G. Dell'Agli, M. Bortolotti, V. M. Sglavo, *J. Mater. Sci*. **2018**, *53*, 8074, https://doi.org/10.1007/s10853-018-2168-9.
[68] T. X. Nguyen, J. Patra, J. K. Chang, J. M. Ting, *J. Mater. Chem. A* **2020**, *8*, 18963, https://doi.org/10.1039/d0ta04844e.
[69] A. Q. Mao, H. Z. Xiang, Z. G. Zhang, K. Kuramoto, H. Y. Yu, S. L. Ran, *J. Magn. Magn. Mater*. **2019**, *484*, 245, https://doi.org/10.1016/j.jmmm.2019.04.023.
[70] S. H. Albedwawi, A. AlJaberi, G. N. Haidemenopoulos, K. Polychronopoulou, *Mater. Des.* **2021**, *202*, https://doi.org/10.1016/j.matdes.2021.109534.
[71] A. Miura, S. Ishiyama, D. Kubo, N. C. Rosero-Navarro, K. Tadanaga, *J. Ceram. Soc. Jpn* **2020**, *128*, 336, https://doi.org/10.2109/jcersj2.20001.
[72] A. Zawisza, A. J. Knorpp, A. H. Clark, D. Kata, T. Graule, M. Stuer, (under revision) **2022**.
[73] P. K. Huang, J. W. Yeh, *Scripta Mater.* **2010**, *62*, 105, https://doi.org/10.1016/j.scriptamat.2009.09.015.
[74] Y. Zhang, W. M. Guo, Z. B. Jiang, Q. Q. Zhu, S. K. Sun, Y. You, K. Plucknett, H. T. Lin, *Scripta Mater.* **2019**, *164*, 135, https://doi.org/10.1016/j.scriptamat.2019.01.021.
[75] D. Yu, B. H. Zhang, J. Yin, Y. C. Wang, X. J. Liu, M. J. Reece, Z. R. Huang, *J. Am. Ceram. Soc.* **2021**, https://doi.org/10.1111/jace.18116.
[76] J. Q. Gao, J. Chen, G. L. Liu, Y. J. Yan, Z. R. Huang, *Int. J. Appl. Ceram. Tec*. **2012**, *9*, 847, https://doi.org/10.1111/j.1744-7402.2011.02671.x.
[77] W. T. Yang, G. P. Zheng, *J. Am. Ceram. Soc.* **2021**, https://doi.org/10.1111/jace.18129.
[78] J. Gild, M. Samiee, J. L. Braun, T. Harrington, H. Vega, P. E. Hopkins, K. Vecchio, J. Luo, *J. Eur. Ceram. Soc*. **2018**, *38*, 3578, https://doi.org/10.1016/j.jeurceramsoc.2018.04.010.
[79] F. Wang, X. Zhang, X. L. Yan, Y. F. Lu, M. Nastasi, Y. Chen, B. Cui, *J. Am. Ceram. Soc.* **2020**, *103*, 4463, https://doi.org/10.1111/jace.17103.
[80] L. Feng, W. G. Fahrenholtz, G. E. Hilmas, *J. Eur. Ceram. Soc*. **2020**, *40*, 3815, https://doi.org/10.1016/j.jeurceramsoc.2020.03.065.
[81] W. Zhang, L. Chen, C. Xu, X. Lv, Y. Wang, J. Ouyang, Y. Zhou, *J. Mater. Sci. Technol*. **2022**, *110*, 57, https://doi.org/10.1016/j.jmst.2021.08.070.
[82] N. X. Zhou, T. Hu, J. J. Huang, J. Luo, *Scripta Mater*. **2016**, *124*, 160, https://doi.org/10.1016/j.scriptamat.2016.07.014.
[83] G. S. Rohrer, *Curr. Opin. Solid St. M*. **2016**, *20*, 231, https://doi.org/10.1016/j.cossms.2016.03.001.
[84] H. Chen, J. Fu, P. F. Zhang, H. G. Peng, C. W. Abney, K. C. Jie, X. M. Liu, M. F. Chi, S. Dai, *J. Mater. Chem. A* **2018**, *6*, 11129, https://doi.org/10.1039/c8ta01772g.
[85] C. Riley, A. De La Riva, J. E. Park, S. J. Percival, A. Benavidez, E. N. Coker, R. E. Aidun, E. A. Paisley, A. Datye, S. S. Chou, *Acs Appl. Mater. Inter*. **2021**, *13*, 8120, https://doi.org/10.1021/acsami.0c17446.
[86] H. Chen, W. W. Lin, Z. H. Zhang, K. C. Jie, D. R. Mullins, X. H. Sang, S. Z. Yang, C. J. Jafta, C. A. Bridges, X. B. Hu, R. R. Unocic, J. Fu, P. F. Zhang, S. Dai, *Acs Mater. Lett.* **2019**, *1*, 83, https://doi.org/10.1021/acsmaterialslett.9b00064.
[87] A. Majumdar, J. Deutch, *Joule* **2018**, *2*, 805, https://doi.org/10.1016/j.joule.2018.04.018.
[88] D. Y. Feng, Y. B. Dong, L. L. Zhang, X. Ge, W. Zhang, S. Dai, Z. A. Qiao, *Angew. Chem. Int. Ed*. **2020**, *59*, 19503, https://doi.org/10.1002/anie.202004892.
[89] C. Deng, P. W. Wu, L. H. Zhu, J. He, D. J. Tao, L. J. Lu, M. Q. He, M. Q. Hua, H. M. Li, W. S. Zhu, *Appl. Mater. Today* **2020**, *20*, https://doi.org/10.1016/j.apmt.2020.100680.
[90] Z. H. Zhang, S. Z. Yang, X. B. Hu, H. D. Xu, H. G. Peng, M. M. Liu, B. P. Thapaliya, K. C. Jie, J. H. Zhao, J. X. Liu, H. Chen, Y. Leng, X. Y. Lu, J. Fu, P. F. Zhang, S. Dai, *Chem. Mater*. **2019**, *31*, 5529, https://doi.org/10.1021/acs.chemmater.9b01244.
[91] M. V. Landau, R. Vidruk, D. Vingurt, D. Fuks, M. Herskowitz, *Rev. Chem. Eng*. **2014**, *30*, 379, https://doi.org/10.1515/revce-2014-0011.
[92] D. Vingurt, D. Fuks, M. V. Landau, R. Vidruk, M. Herskowitz, *Phys. Chem. Chem. Phys*. **2013**, *15*, 14783, https://doi.org/10.1039/c3cp51086g.
[93] A. Amiri, R. Shahbazian-Yassar, *J. Mater. Chem. A* **2021**, *9*, 782, https://doi.org/10.1039/d0ta09578h.
[94] N. Nitta, F. X. Wu, J. T. Lee, G. Yushin, *Mater. Today* **2015**, *18*, 252, https://doi.org/10.1016/j.mattod.2014.10.040.
[95] K. Mizushima, P. C. Jones, P. J. Wiseman, J. B. Goodenough, *Mater. Res. Bull*. **1980**, *15*, 783, https://doi.org/10.1016/0025-5408(80)90012-4.
[96] A. Sarkar, L. Velasco, D. Wang, Q. S. Wang, G. Talasila, L. de Biasi, C. Kubel, T. Brezesinski, S. S. Bhattacharya, H. Hahn, B. Breitung, *Nat. Commun*. **2018**, *9*, https://doi.org/10.1038/s41467-018-05774-5.
[97] J. Chen, W. X. Liu, J. X. Liu, X. L. Zhang, M. Z. Yuan, Y. L. Zhao, J. J. Yan, M. Q. Hou, J. Y. Yan, M. Kunz, N. Tamura, H. Z. Zhang, Z. L. Yin, *J. Phys. Chem. C* **2019**, *123*, 17735, https://doi.org/10.1021/acs.jpcc.9b04992.
[98] C. Oses, C. Toher, S. Curtarolo, *Nat. Rev. Mater.* **2020**, *5*, 295, https://doi.org/10.1038/s41578-019-0170-8.
[99] N. Qiu, H. Chen, Z. M. Yang, S. Sun, Y. Wang, Y. H. Cui, *J. Alloy Compd*. **2019**, *777*, 767, https://doi.org/10.1016/j.jallcom.2018.11.049.
[100] D. Berardan, S. Franger, A. K. Meena, N. Dragoe, *J. Mater. Chem. A* **2016**, *4*, 9536, https://doi.org/10.1039/c6ta03249d.
[101] D. Berardan, S. Franger, D. Dragoe, A. K. Meena, N. Dragoe, *Phys. Status Solidi-R* **2016**, *10*, 328, https://doi.org/10.1002/pssr.201600043.
[102] D. Berardan, A. K. Meena, S. Franger, C. Herrero, N. Dragoe, *J. Alloy Compd.* **2017**, *704*, 693, https://doi.org/10.1016/j.jallcom.2017.02.070.
[103] T. Jin, X. H. Sang, R. R. Unocic, R. T. Kinch, X. F. Liu, J. Hu, H. L. Liu, S. Dai, *Adv. Mater*. **2018**, *30*, https://doi.org/10.1002/adma.201707512.

[104] S. Walia, S. Balendhran, H. Nili, S. Zhuiykov, G. Rosengarten, Q. H. Wang, M. Bhaskaran, S. Sriram, M. S. Strano, K. Kalantar-zadeh, *Prog. Mater. Sci*. **2013**, *58*, 1443, https://doi.org/10.1016/j.pmatsci.2013.06.003.
[105] Y. N. Yin, B. Tudu, A. Tiwari, *Vacuum* **2017**, *146*, 356, https://doi.org/10.1016/j.vacuum.2017.04.015.
[106] Z. L. Ouyang, D. W. Li, *Sci. Rep. UK* **2016**, *6*, https://doi.org/10.1038/srep24123.
[107] D. M. Rowe, 'CRC Handbook of Thermoelectrics', First edition. ed., CRC Press, Boca Raton, FL, **1995**.
[108] H. Y. Zhu, Y. Li, H. T. Li, T. C. Su, C. Y. Pu, Y. S. Zhao, Y. M. Ma, P. W. Zhu, X. Wang, *High Pressure Res*. **2017**, *37*, 36, https://doi.org/10.1080/08957959.2016.1273352.
[109] S. Paengson, P. Pilasuta, K. Singsoog, W. Namhongsa, W. Impho, T. Seetawan, *Mater. Today-Proc*. **2017**, *4*, 6289, https://doi.org/10.1016/j.matpr.2017.06.129.
[110] R. Banerjee, S. Chatterjee, M. Ranjan, T. Bhattacharya, S. Mukherjee, S. S. Jana, A. Dwivedi, T. Maiti, *Acs Sustain. Chem. Eng.* **2020**, *8*, 17022, https://doi.org/10.1021/acssuschemeng.0c03849.
[111] M. V. Feigelman, V. B. Geshkenbein, A. I. Larkin, *Physica C* **1990**, *167*, 177, https://doi.org/10.1016/0921-4534(90)90502-6.
[112] B. Keimer, S. A. Kivelson, M. R. Norman, S. Uchida, J. Zaanen, *Nature* **2015**, *518*, 179, https://doi.org/10.1038/nature14165.
[113] A. Sarkar, R. Kruk, H. Hahn, *Dalton Trans*. **2021**, *50*, 1973, https://doi.org/10.1039/d0dt04154h.
[114] P. B. Meisenheimer, T. J. Kratofil, J. T. Heron, *Sci. Rep. UK* **2017**, *7*, https://doi.org/10.1038/s41598-017-13810-5.

License and Terms

The definitive version of this article is the electronic one that can be found at https://doi.org/10.2533/chimia.2022.212